

Microstructure and shear strength of ZrB₂-SiC/Ti-6Al-4V joint by TiCuZrNi with Cu foam

Gang Wang^{1,*}, Zhentao Wang¹, Wei Wang², Rujie He^{3,*}, Kaixuan Gui¹, Caiwang
Tan⁴, Wei Cao^{5,1}

¹ School of Mechanical and Automotive Engineering, Anhui Polytechnic University,
Wuhu 241000, PR China

² School of Mechanical Engineering, Anhui Machine and Electricity College, Wuhu
241002, PR China

³ Institute of Advanced Structure Technology, Beijing Institute of Technology, Beijing
100081, PR China

⁴ State Key Laboratory of Advanced Welding and Joining, Harbin Institute of
Technology, Harbin 150001, PR China

⁵ Nano and Molecular Systems Research Unit, University of Oulu, P.O. Box 3000,
FIN-90014, Oulu, Finland

Correspondence: herujie@bit.edu.cn; gangwang@ahpu.edu.cn

Abstract

In this paper, brazing behaviors between ZrB₂-SiC and Ti-6Al-4V by Cu foam interlayer were studied. The microstructure, formation mechanism, mechanical property and fracture surface of the joints were systematically studied. Results showed phases in the joints were $\alpha+\beta$ -Ti, TiCu, Ti₂Cu, Cu(s, s), TiC, TiB₂ and Ti₃SiC₂. An optimum shear strength reached up to 435MPa at a brazing temperature of 910 °C and holding time of 20 min. Such a shear strength was 90 MPa higher than the one without the Cu foam. The high shear strength bears impacts from microstructure and residual stress. With the increase of brazing time, Cu(s,s) gradually disappeared and the content of Ti₂Cu intermetallic compound increased, which was harmful for the joint. Furthermore, the residual stress of joint with Cu foam was calculated to 324 MPa, lower than the one without Cu foam interlayer.

Keywords: UHTC; brazing; microstructure; shear strength; Cu foam

1. Introduction

ZrB₂-SiC ceramics (named as ZS for convenience) are advantageous to their thermal protection ability for sharp parts in aerospace and spacecraft applications thanks to their high melting temperatures, excellent oxidation and thermal shock resistances, and superior chemical stabilities [1-3]. However, due to their poor machinability and brittle character, it is difficult to process such ceramics into components with complicated shapes. To overcome this drawback, the ZS ceramics have been proposed to connect to other materials. Till now, various techniques have been attempted to joining the ceramics, such as brazing [4-7], diffusion bonding [8] and transient liquid phase bonding [9, 10]. Among these techniques, brazing is a low-cost and simple method to join materials, especially dissimilar materials. Singh and Asthana reported successful joining of ZS ceramics by Ni-based metallic glass, Pd- and Ag- filler. Sciti *et al.* studied the weldability of the ZS ceramics by using CaAlSiO glass as filler, and obtained a joint with a good strength of 277 MPa at room temperature [11]. Yuan *et al.* successfully brazed ZS/ZS using pure Ni powders as an interlayer, and the brazed joint exhibited a maximum shear strength of 60 MPa [12]. Li *et al.* used Ti-based powder filler metal to braze ZS. At 917°C for 10 min, a satisfactory mechanical performance was obtained with the strength of 143.5 MPa [13]. It has been reported that ZS ceramics could be joined to themselves and TC4 alloy by Ag-, Cu- and Ni-based fillers [14, 15]. The maximum strength reached up to 74 MPa. ZS ceramics could also be brazed to GH99 superalloy with the help of a Ti-modified FeCoNiCrCu alloy and the effect of the filler on microstructure evolution of ZS /GH99 joint was also verified [16]. In our previous work, TiCuZrNi filler was used for ZS/ZS and ZS/TC4 brazing. The joint possessed a stable strength of 240 MPa at a high temperature of 600°C [17, 18]. However, this joint suffered from harmful

mismatches between the ceramic and the metal due to the inhomogeneous thermal residual stresses among the joint, as a result of different coefficients of thermal expansion (CTE). The thermal residual stress among the brazed joints thus should be released.

Typically, thermal residual stress of joints can be reduced by introducing low CTE materials [19-21], soft metal foil interlayer [22, 23], powders [24-26], and foam metals [27-35] and so on. However, additive powders might cause poor distribution at the joint and result in uncontrollable reinforcement effect. Metal foil introduces a new interface between the filler and the foil where cracks can easily propagate. Compared with traditional metal foil, metal foam is more effective to release thermal residual stress. Yang *et al* reported that ZS ceramics were diffusively joined to Nb by Ni foam. When using Ni foam with a thickness of 4 mm as the interlayer, the shear strength of the joints was 155.6 MPa [36]. Zaharinie *et al.* introduced a porous Cu/Ni composite as an interlayer to braze sapphire ceramic and Inconel 600 alloy for pressure sensor applications [37]. Wang *et al* introduced an interlayer of Cu foam to increase the brazing strength at the joints, which reached up to 84.5 MPa, 95 % higher than that without Cu foam interlayer [38]. A composite interlayer of carbon-covered Cu foam was found helpful for the formation of TiC when brazing C/C composite and Nb [39]. The joint could be therefore strengthened.

Based on our previous studies of ZS/ZS and ZS/TC4 brazing [17, 18], in this work, Cu foam was used as an interlayer to braze ZS ceramics and TC4 using TiCuZrNi filler alloy to release thermal residual stress among the joints. Detailed impacts of brazing parameters and influences of the Cu foam on microstructure and mechanical properties of the ZS/TC4 joint were also discussed.

2. Experimental

Commercial ZrB₂ powder (Beijing Zhongjinyan Micropowder Co. Ltd., Beijing, China) and SiC powder (Weifang Kaihua Micro-powder Co. Ltd., Weifang, China) were used as the raw materials. The ZrB₂ powder had a purity above 99% and particle size of 2 μm. The SiC powder was predominantly α-SiC with a purity of 99% and particle size of 1 μm. The powders were batched at a ratio of 80 vol% ZrB₂ to 20 vol% SiC. The powder mixture was ball milled in ethanol for 8 h with zirconia ball media in a planetary mill (MCA-10B, Nanjing Nanda Instrument Plant Co. Ltd., China) at 240 rpm (revolutions per minute). After ball-milling, ethanol was removed by a rotating evaporator (R-202, Shanghai Shensheng Biotech Co. Ltd., China) at 80 °C to minimize segregation. The as-received ZS powder mixtures were sieved through a 200 mesh to obtain homogeneous powder mixtures and then uniaxially hot-pressed in a BN coated graphite die at 1950°C for 60 min under vacuum and 30 MPa applied pressure (ZT-70-23Y, Shanghai Chenxin Furnace Co., Ltd., China).

The CTE was measured by using a standard thermal expansion instrument (NETZSCH DIL, 402C, Germany). Table 1 shows the average CTE of the ZS ceramic at different temperatures. A commercial TC4 alloy plate was used in the present work. Both ZS and TC4 samples were cut into 4 mm × 4 mm × 4 mm for brazing. Ti_{30.21}Cu_{41.83}Zr_{19.76}Ni_{8.19} (at. %) amorphous filler metal with a thickness of 30 μm was used in this study. The filler was prepared by single roller-spinning technique, and the amorphous structure was examined by an X-ray diffraction [17]. The Cu foams with a thickness of 0.5 mm was used as the interlayer. Fig. 1a shows the morphology of the Cu foam. The average pore size and porosity of Cu foams are ~400 μm and ~80%, respectively.

Before brazing, the surfaces of the ZS and TC4 were carefully ground and

polished. All the materials, including Cu foams and filler foils were ultrasonically cleaned in alcohol for 10 min. Fig. 1b shows that the Cu foam and filler foils were sandwich layered by the ZS and TC4. The brazing was done at 910°C for 10, 20 or 50 min, respectively, under a vacuum of 1×10^{-3} Pa with a heating rate 10°C/min, respectively.

Scanning electron microscopy (SEM, SU-8010) with an energy-dispersive X-ray spectrometer (EDS) was employed to study the microstructure of the joints and the fracture surface. An Instron 5500 testing machine was used for shear testing. During the testing, three samples for each brazing parameters were tested to obtain an average value.

Table 1 CTE of the ZrB₂-SiC ceramic at different temperatures.

Temperature(°C)	25~300	300~500	500~800	800~1000
CTE($10^{-6}/^{\circ}\text{C}$)	4.07	4.65	5.79	6.46

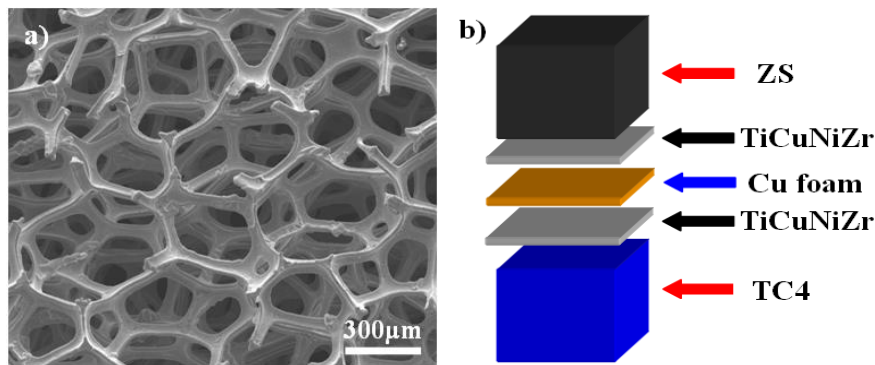


Fig.1 a) Microstructure of Cu foam, and b) schematic diagram of brazing assembly.

3. Results and discussion

The microscopy of ZS ceramic, ZS/TC4 joint with the Cu foam, and corresponding EDS results of the joint are shown in Fig. 2. In the SEM micrograph of

the polished surfaces of the sintered ZS ceramic (Fig.2a), the dark particle phase is identified as SiC, which is uniformly dispersed in the gray ZrB₂ matrix, as the same from Ref [7]. The microstructure of the ceramic is regular, and no obvious pores are observed. Similarly, no crack or pore at the joint part was observed in Fig. 2b. Here Cu foam was used and the joint was brazed at 910°C for 600 s. The thickness of joint was ~150 μm, smaller than that of Cu foam. Cu foam had a large porosity (Fig.1a), and was easily compressed and filled during brazing. Therefore, 0.5 mm thick Cu foam could be compressed into only ~150 μm after brazing. Ti and Cu were massively diffused and distributed in the whole joint, as shown in Fig.2c and 2d. Ti and Cu were crucial for the joining of ZS/TC4. Zr was mainly distributed in the ZS side, as shown in Fig. 2e. In Fig.2f, Ni was found to distribute in the whole brazing seam. Al and V elements in the TC4 alloy also diffused into the joint, as shown in Fig. 2g and 2h. B and Si elements were mainly diffused in the ZS side after migration from the ZS ceramic, as shown in Fig. 2i and 2j. From Fig.2k, it was found that C was homogeneous in the brazed joint, suggesting an excellent diffusion rate of the C.

Figure 3a shows a typical microstructure of the ZS/TiCuZrNi/Cu foam/TiCuZrNi/TC4 joint brazed at 910°C for 20 min. A smooth joint without any defect could be obtained with Cu foam interlayer. Two continuous reaction layers were detected in both ZS and TC4 sides. In addition to the brazing seam, there were also three types of reaction zones observed in the whole joint, i.e., TC4/brazing filler metal diffusion layer, center zone and brazing filler metal/ZS diffusion layer, signed as zone I, II and III, respectively. For comparison purpose, the interfacial microstructure of the joint brazed without Cu foam was presented in Fig. 3b [18]. It could also be divided into three zones, denoted as 1, 2 and 3, respectively. From the whole view, difference between Fig.3a and Fig.3b was mainly found at the

microstructure of center zone of the joint. There were many discontinuous blocky gray structures and eutectic structure in the Fig.3a with Cu foam. However, center zone of joint without Cu foam was almost all composed of Ti-Cu eutectic structure, as shown in Fig. 3b. Figures 3c, 3d and 3e demonstrated the high magnification images of I, II, and III characteristic zones of Fig. 3a, respectively.

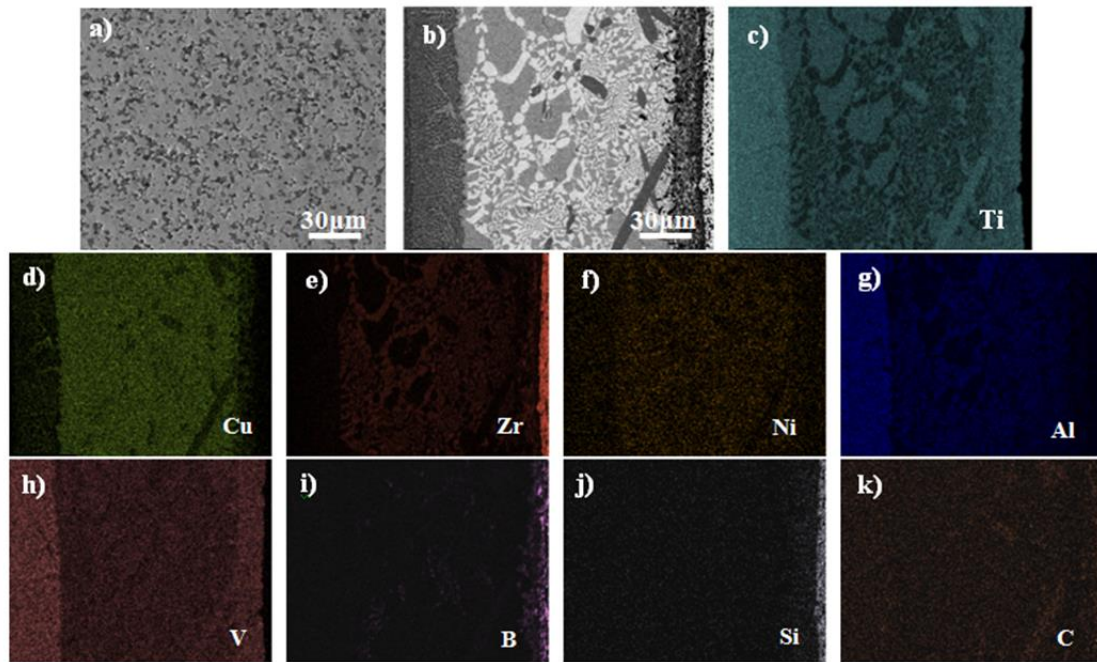


Fig. 2 a) Typical microstructure of ZS materials b) interfacial microstructure, and elemental distribution of c)Ti, d)Cu, e) Zr, f)Ni, g)Al, h)V, i)B, j)Si, k)C elements in the brazed joint.

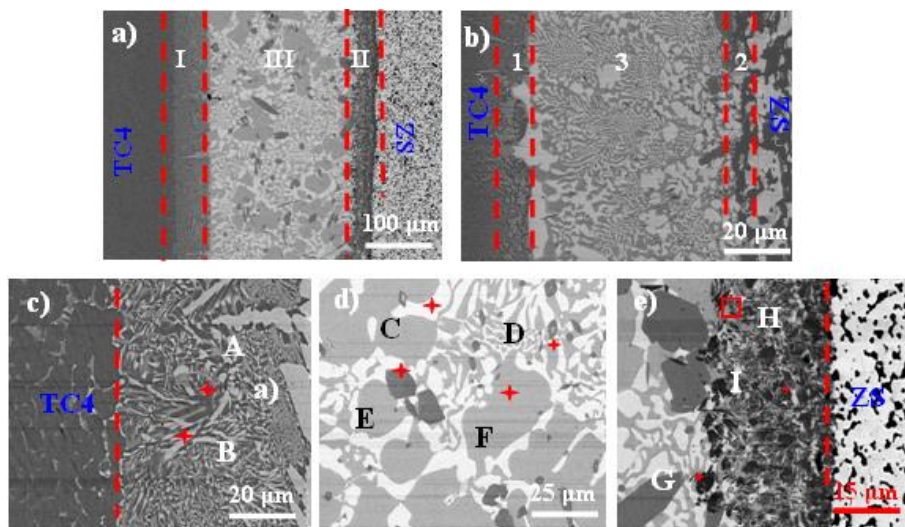


Fig.3 SEM images of the brazed joint a) with Cu foam, b) without Cu foam,

c) zoomed image of I zone, d) magnification images of II zone, and e) zoomed image of III zone.

The joint region owns different phases marked as A-I whose chemical compositions were analyzed by EDS and listed in Table 2. The regions of A and B were mainly Ti, and were formed close to TC4. The elements of Cu and Ni were reported as the stabilizer for β -Ti [40]. Thus, it was possible for α -Ti to transform into β -Ti in the TC4 side. This leads to the formation of many β -Ti phases. Therefore, points A and B can be defined as α -Ti and β -Ti, respectively. The atomic ratio of Ti and Cu of the white point C in the zone II was approximately 1:1. Similarly, the Ti and Cu ratio at point D was 2:1. According to the Ti-Cu binary diagram and Ref. [41], points C and D were considered as TiCu phase and Ti₂Cu phase, respectively. They were formed in a eutectic reaction of $L \rightarrow \text{TiCu} + \text{Ti}_2\text{Cu}$. The region of point E in zone III was mainly Ti and C elements. From the ratio of elements, it was identified as TiC. TiC was yielded from the Ti and C ($\text{Ti} + \text{C} \rightarrow \text{TiC}$). Since the Gibbs free energy for TiC formation was negative, TiC was formed from an *in situ* reaction [39]. The blocky gray phase (Point F) was mainly composed of Cu, which is inferred as Cu-based solid solution (Cu(s, s)). Most of the blocky Cu(s, s) are originated from the Cu foam. For the black phase of point G from Fig.3e, the atomic ratio of C and Ti for point was 1:1. The square position of H was mainly composed of Ti, C and B, and white phase of point I of Ti, C, B and Si. During the brazing process, Ti was more likely to react with SiC [42], resulting in the formation of Ti₃SiC₂ ($\text{Ti} + \text{SiC} \rightarrow \text{Ti}_3\text{SiC}_2$). The remaining Ti reacted with ZrB₂, leading to the TiB₂ phases ($\text{Ti} + \text{ZrB}_2 \rightarrow \text{TiB}_2 + \text{Zr}$). The phases could be identified by the chemical compositions, phase diagrams and previous reports [18, 38, 42]. The phases A to I were α -Ti, β -Ti, TiCu, Ti₂Cu, TiC, Cu(s,s), TiC, TiB₂+TiC and TiB₂+Ti₃SiC₂, which were summarized in Table 2.

Table 2 EDS of each point marked in Fig. 3.

Point	Ti	Cu	Zr	Ni	Al	V	B	Si	C	Possible phase
A	72.2	1.1	0.17	0.88	10.5	2.61	0.64	0.29	11.62	α -Ti
B	58.85	8.22	0.59	0.91	9.85	5.58	0.58	0.39	15.02	β -Ti
C	26.72	26.01	6.58	2.83	10.73	2.29	5.26	0.92	8.66	TiCu
D	52.50	26.5	1.39	1.46	5.07	2.38	1.80	0.61	8.24	Ti ₂ Cu
E	41.34	7.91	0.96	0.66	5.00	1.45	1.97	1.29	39.41	TiC
F	18.58	70.66	1.54	1.41	0.16	0.17	0.94	0.63	4.91	Cu(s,s)
G	41.96	0.35	1.57	0.4	1.41	1.48	7.19	2.42	43.22	TiC
H	34.61	1.18	0.64	0.44	1.19	3.28	44.22	0.23	14.22	TiB ₂ +TiC
I	30.00	0.49	5.57	0.4	1.09	1.7	25.83	8.07	26.85	TiB ₂ +Ti ₃ SiC ₂

Based on the analysis above, we propose the following formation mechanism of the brazed ZS/TC4 joint and the diagram is drawn in Fig.4:

1) With the increase of temperature, the TiCuZrNi fillers and Cu foam were plastically deformed and tightly contact each other, as shown in Fig. 4a. When the temperature approaches the melting point of the filler, the molten filler alloy wets the surface of the base materials, and fills the pore of the Cu foam. Simultaneously, parts of the base materials are also dissolved into the molten alloy. The main elements of Ti, Cu, Zr, Ni, B, C and Si start to diffuse, as shown in Fig. 4b.

2) Continuously increasing the temperature leads to a large number of Ti atoms diffuses from TiCuZrNi filler and TC4 to the ZS side. Firstly, ternary phase of Ti₃SiC is precipitated through the reaction of $\text{Ti} + \text{SiC} \rightarrow \text{Ti}_3\text{SiC}$. Then the TiC is also formed following $\text{Ti} + \text{C} \rightarrow \text{TiC}$, as shown in Fig.4c. For TC4 side, the diffusion of Cu atoms from TiCuZrNi filler into TC4 alloy decrease the allotropic transformation temperature of α -Ti to β -Ti [43], resulting in the formation of many β -Ti, as shown in Fig.4c. During this process, the molten filler metal partially fills into the pore of Cu

foam, and Cu foam is pressed.

3) Further increasing temperature to the brazing temperature yields continuous infiltrations of the molten filler metal into the Cu foam and weld width reduction. The Ti element either from the rest of the filler or diffused from TC4 alloy can react with the B at the ZS side. The TiB_2 is formed by $Ti + B \rightarrow TiB_2$ at the same side, as shown in Fig.4d. In the middle of the joint, $TiCu$ and Ti_2Cu phases are mainly formed by the eutectic reaction of $L \rightarrow TiCu + Ti_2Cu$. It was reported that the Gibbs free energy of the $TiCu$ was lower than that of the Ti_2Cu [44]. Thus, the $TiCu$ was precipitated before the Ti_2Cu via the reaction of $Ti + Cu \rightarrow TiCu$. As a result, the $TiCu$ phase owns a larger fraction than Ti_2Cu phase, as shown in Fig. 3d. In the TC4 side, more and more β -Ti are formed via the α -Ti $\rightarrow\beta$ -Ti transformation. Meanwhile, due to the diffusion of C, some TiC particles are formed in the middle of the joint (Fig. 4d).

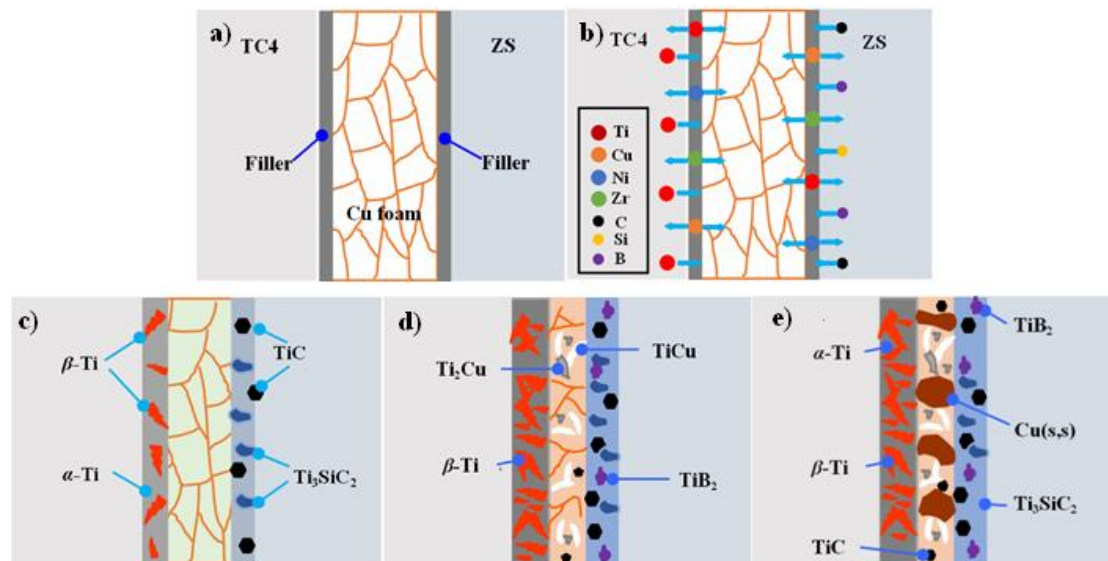


Fig.4 Microstructural evolution of the ZS/TC4 brazed joints with Cu foam as interlayer: a) and b) the interaction between brazing filler and base materials; c) and d) the phase formation in the joint; e) the solidification stage of joint.

4) Below the β - α transformation temperature a the cooling process, the β -Ti

phase is decomposed to $\alpha+\beta$ Ti in the TC4 side. Ti element from TC4 and metal filler diffuse into the Cu foam and form Cu(s, s). The Cu foam keeps its three-dimensional (3D) structure.

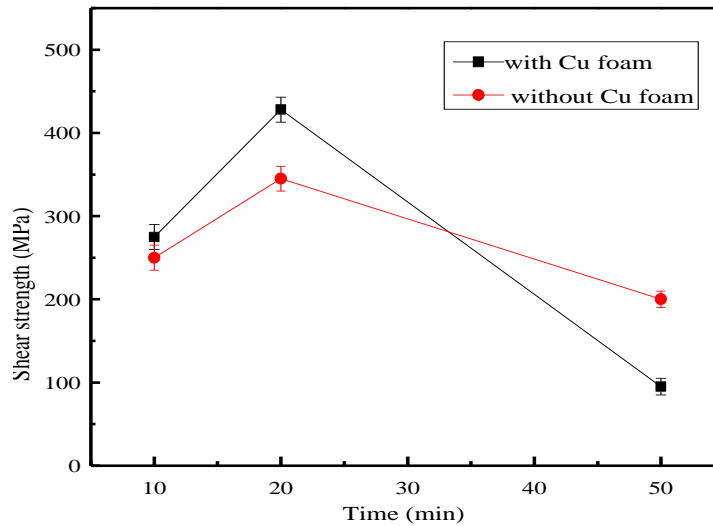


Fig.5 The shear strengths of the brazed joint as a function of brazing time.

Figure 5 depicts the shear strength of the ZS/TC4 brazed joints with and without Cu foam [18] for different holding times at 910 °C. The shear strength reaches a maximum value of 435 MPa, 90 MPa higher than that without the Cu foam. This suggests that the Cu foam interlayer significantly improves the mechanical properties. Afterwards the strength decreases to 95 MPa at a holding time of 50 min.

The microstructural impacts on the shear strength of the joint were investigated. Figure 6 shows the microstructure of joints with Cu foam interlayer for different holding times at 910°C. Generally speaking, in case of Cu foam with a thickness of 0.5 mm, the microstructure of joint significantly changed with the increase of brazing time. The composition of the blocky gray phase in the brazing seam with different brazing parameters was detected by EDS, as shown in Table 3. With prolongation of the holding time, Cu(s,s) gradually diminished and the Ti-Cu intermetallic compound turned out. At a 10 min holding time, a small amount of Ti-Cu eutectic phase and

many of Cu(s, s) turned out in the joint, as shown in Fig.6a. In this condition, Cu foam still kept the 3D structure. With the brazing time increased to 20 min, the amount and size of Cu (s, s) slightly decreased. Ti-Cu eutectic structure (TiCu and Ti₂Cu) became thicker, as shown in Fig.6b. However, under this condition, the 3D structure of the Cu foam was still kept in the joint. On one hand, it was reported that the Cu foam had a good energy absorption capacity. The filling metal permeated the gap of Cu foam to produce staggered structure [37]. This mechanism was constructive to improve the bonding strength of interfaces, thus improving the mechanical properties of joints. It is worth noting that the TiC particles are dispersed and distributed as a reinforcement phase in the joint. This is beneficial to strengthen the joint [39]. Further increase of the brazing time to 50 min thickened the $\alpha + \beta$ -Ti layer in the TC4 side and reaction layer in ZS ceramics side. However, the width of the joint was reduced, because of the collapse of the Cu foam for a long brazing time. The amount of Cu(s, s) almost vanished. TiCu and Ti₂Cu eutectic phases take a large portion in the joint, as shown in Fig. 6c. This phenomenon is explained as follows. When the holding time reached 50 min, more Ti are dissolved and diffused from TC4 and TiCuZrNi filler metal. The Ti reacted with Cu from the filler metal and the Cu foam. Under this condition, the Cu foam in the joint was almost completely consumed by the Ti-Cu reaction. Ti-Cu compounds grew rapidly and went cross distributed. The large amount of Ti-Cu intermetallic compound may cause strong hardening effect and reduce the ductility and therefore becomes detrimental for the joint strength [45, 46].

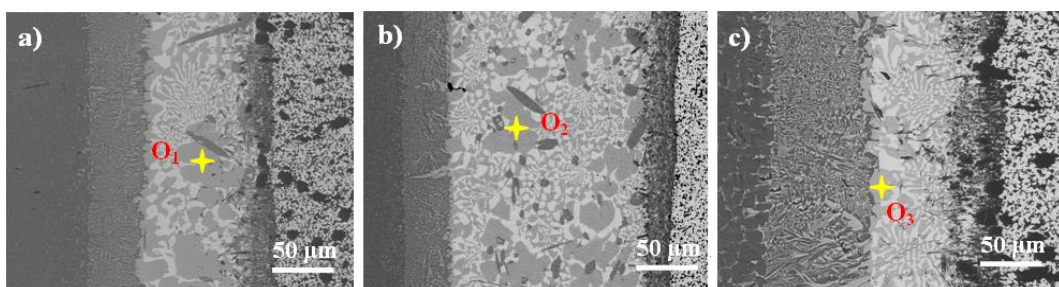


Fig. 6 Interfacial microstructure of the ZS/TC4 brazed joints with Cu foam at 910°C for different holding times: a) 10 min; b) 20min, and c) 50 min.

Table 3 EDS of the blocky structure with different brazing parameters

Point	Ti	Cu	Zr	Ni	Al	V	B	Si	C	Possible phase
O ₁	15.93	70.32	1.92	2.24	2.73	2.53	1.11	0.87	2.35	Cu(s,s)
O ₂	24.35	64.01	2.63	2.91	0.24	1.90	1.50	0.30	5.16	Cu(s,s)
O ₃	51.72	27.06	5.26	3.24	4.79	1.96	1.28	0.30	8.16	Ti ₂ Cu

The shear strength is also influenced by the residual stress caused by CTE difference between the metal and the ceramic. The residual stress only with TiCuZrNi filler can be simply calculated as [47]:

$$\sigma = \frac{E_c E_m}{E_c + E_m} (\alpha_c - \alpha_m) \Delta T \quad (1)$$

where σ is the residual stress in the joint, E_m and E_C the elastic modulus of TiCuZrNi filler and ZS ceramic. α_c and α_m are the CTE of the ZS ceramic and TiCuZrNi filler. ΔT is the difference between brazing temperature and room temperature. From Ref. [48] and Table 1, the data of ZS ceramic and TiCuZrNi filler can be approximately obtained. At the joining temperature, E_C and E_m are estimated to 320 and 120 GPa, respectively, and α_c and α_m to 6.46×10^{-6} and $10.7 \times 10^{-6}/^\circ\text{C}$, respectively. Considering the room temperature as 20°C, ΔT is 890°C. Based on Eq. (1), the residual stress σ in the ZS side is calculated to 354 MPa.

When the Cu foam is introduced, the filler can be considered as a composite system. It contains the Cu foam and TiCuZrNi filler, and the elastic modulus of this composite filler system is estimated as follows [49]:

$$E_s = a^2 E_{Cu} + (1-a)^2 E_m + \frac{2a(1-a)E_{Cu}E_m}{aE_{Cu} + (1-a)E_m} \quad (2)$$

where a is a constant related to the porosity of the Cu foam. E_s , E_{Cu} and E_m are the elastic modulus of the composite filler system, Cu foam (110 GPa) and TiCuZrNi filler (135 GPa), respectively. a is 0.3 at a 80% Cu porosity [32]. Thus, E_s is calculated to 114 GPa.

The CTE of the composite filler system was reported as follows [50]:

$$\alpha_s = \frac{\frac{V_m K_m \alpha_m}{d_m} + \frac{V_{Cu} K_{Cu} \alpha_{Cu}}{d_{Cu}}}{\frac{V_m K_m}{d_m} + \frac{V_{Cu} K_{Cu}}{d_{Cu}}} \quad (3)$$

Here α_s , α_{Cu} and α_m are the CTEs of composite filler system, Cu-foam and TiCuZrNi filler, and V_{Cu} and V_m the volumes of Cu foam and TiCuZrNi filler, respectively. In the formula, K_m and K_{Cu} are the bulk modulus of TiCuZrNi filler and Cu foam, while d_m and d_{Cu} the density of TiCuZrNi filler and Cu foam.

The relation of E (elastic modulus), K (bulk modulus) and G (shear modulus) are described by:

$$G = \frac{E}{2(1+\nu)} \quad (4)$$

$$K = \frac{E}{3(1-2\nu)} \quad (5)$$

where ν was the poisson ratio. A Cu foam of 80 % porosity yielded 0.8 for the $V_m/(V_{Cu}+V_m)$ ratio. Based on the above analysis and calculation, α_s is calculated to $10.9 \times 10^{-6}/^\circ\text{C}$. According to Eq. (1), in the presence of Cu foam interlayer, the residual stress in the ZS side is found to ~324 MPa, a little smaller than that without Cu foam (354 MPa). So, it can be found that in the present work the CTE of the composite filler system is similar to that of the TiCuZrNi filler, indicating that the change in the CTE of the filler is not a key factor altering the joint properties.

Figure.7 shows the fracture morphology of brazed joints at the ZS ceramic side

without and with Cu foam interlayer at 910°C for 20 min. In the absence of Cu foam interlayer, the fracture surface contains two kinds of zones: the reaction layer zone and the ZS ceramics, as shown in Fig.7a. It is shown that the crack emerged in the reaction layer and then propagated into the ZS ceramics. Fig. 7b showed the fracture surface with Cu foam interlayer. Obviously, the fracture of joint only happens at the ZS ceramic side, which indicates that the Cu foam efficiently releases residual stress of the joint.

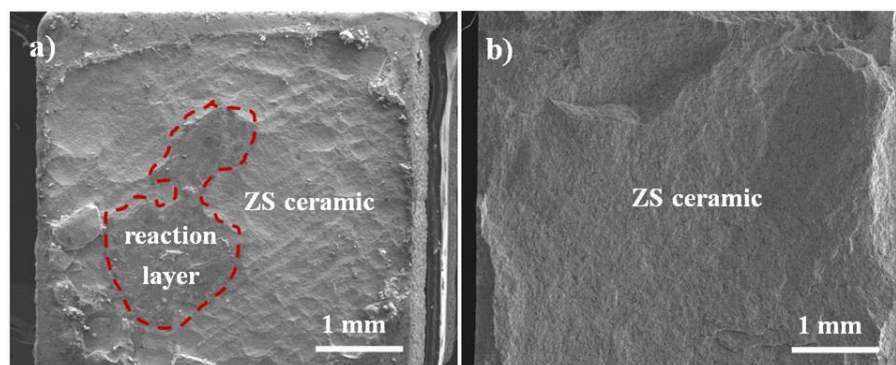


Fig. 7 Fracture morphology of the brazed joints: a) without and b) with Cu foam

4. Conclusions

In this present work, a composite filler system containing TiCuZrNi amorphous alloy and Cu foam was introduced to join ZrB₂-SiC/TC4 together. The interfacial microstructure, mechanical properties and formation mechanism of the joints were investigated in details, and the effects of Cu foam on shear strength were explained from the microstructure and residual stress of the joint. The main conclusions of this present study are drawn as follows:

- 1) A sound joint was achieved at 910°C for different holding times with Cu foam. The interfacial microstructures of the joint were typically composed of TC4 alloy/ $\alpha+\beta$ -Ti/ TiCu/Ti₂Cu/Cu(s, s)/TiC/TiB₂+Ti₃SiC₂/ZS ceramic.
- 2) The shear strength of the joint reached to the maximum value of 435 MPa at

910°C for 20 min. The strength decreased after further increase of the holding time.

3) The Cu (s, s) in the joint decreased significantly with holding time. Ti reacted with Cu from both the filler metal and the Cu foam, resulting in more Ti₂Cu intermetallic compound. They grew rapidly and went cross distributed. The Cu foam in the joint was totally consumed by Ti-Cu reaction. The high content of brittle Ti₂Cu intermetallic compound is harmful for the joint strength.

4) The residual stress of the joint with Cu foam is calculated to 324 MPa, lower than the value of 354 MPa for the condition without Cu foam.

Acknowledgement

This work was financially supported by the National Natural Science Foundation of China [51704001 and 51772028], Natural Science Foundation of Anhui Province [KJ2018A0860, KJ2018A0113, 1508085SQE210, and gxyqZD2016126], Talent Project of Anhui Polytechnic University [2017yyzr08] and the Open Fund of State Key Laboratory of Advanced Welding and Joining [AWJ-16-M04], and the Academy of Finland [311934].

References

- [1] X.H. Zhang, P. Hu, J.C. Han, Structure evolution of ZrB₂-SiC during the oxidation in air, *J. Mater. Res.* 23(2008) 1961–1972.
- [2] Z.L. Qu, R.J. He, X.M. Cheng, D.N. Fang, Fabrication and characterization of B₄C-ZrB₂-SiC ceramics with simultaneously improved high temperature strength and oxidation resistance up to 1600°C, *Ceram. Int.* 42 (2016) 8000-8004.
- [3] X.Y. Tian, J.C. Feng, J.M. Shi, H.W. Li, L.X. Zhang, Brazing of ZrB₂-SiC-C ceramic and GH99 superalloy to form reticular seam with low residual stress. *Ceram. Int.* 41 (2015) 145-153.
- [4] X.R. Song, H.J. Lin, X.R. Zeng, L.L. Zhang, Brazing of C/C composites to Ti6Al4V using graphene nano-platelets reinforced TiCuZrNi brazing alloy. *Mater. Lett.* 183(2016) 232-235.
- [5] M. Singh, R. Asthana. Joining of zirconium diboride-based ultra high-temperature ceramic composites using metallic glass interlayers. *Mater. Sci. Eng A* 460-461 (2007) 153-162.

- [6] R. Asthana, M. Singh. Joining of ZrB₂-based ultra-high-temperature ceramic composites using Pd-based braze alloys. *Scr. Mater.* 61 (2009) 257-260.
- [7] M. Singh, R. Asthana. Joining of ZrB₂-based ultra-high-temperature ceramic composites to Cu-Clad-Molybdenum for advanced aerospace applications. *Int. J. Appl. Ceram. Technol.* 6(2) (2009) 113-133.
- [8] A. Amirnasi, N. Parvin, M. Shafieihaghshenas, Dissimilar diffusion brazing of WC-Co to AISI 4145 steel using RBCuZn-D interlayer, *J. Manuf. Processes.* 28(2017):82–93.
- [9] L. Esposito, D. Sciti, L. Silvestroni, C. Melandri, S. Guicciardi, N. Saito, K. Nakashima, A.M. Glaeser, Transient liquid phase bonding of HfC-based ceramics, *J. Mater. Sci.* 49 (2014) 654-664.
- [10] N. Saito, H. Ikeda, Y. Yamaoka, A.M. Glaeser, K. Nakashima. Wettability and transient liquid phase bonding of hafnium diboride composite with Ni–Nb alloys, *J. Mater. Sci.* 47(2012) 8454-8463.
- [11] D. Sciti, A. Bellosi, L. Esposito, Bonding of zirconia to superalloy with the active brazing technique, *J. Eur. Ceram. Soc.* 21(2001)45–52.
- [12] B. Yuan, G.J. Zhang. Microstructure and shear strength of self-joined ZrB₂ and ZrB₂-SiC with pure Ni. *Scr. Mater.* 64(2011)17-20.
- [13] Z.R. Li, Z.Z. Wang, G.D. Wu, J.C. Feng, Microstructure and mechanical properties of ZrB₂-SiC ultra high temperature ceramic composite joint using TiZrNiCu filler metal, *Sci. Technol. Weld. Join.* 16(2011) 697-701.
- [14] F. Valenza, C. Artini, A. Passerone, M.L. Muolo, ZrB₂-SiC/Ti6Al4V joints: wettability studies using Ag- and Cu-based braze alloys, *J. Mater. Sci.* 47(2012) 8439–8449.
- [15] F. Valenza, C. Artini, A. Passerone, P. Cirillo, M.L. Muolo, Joining of ZrB₂ ceramics to Ti6Al4V by Ni-Based interlayers. *J. Mater. Eng. Perform.* 23(2014) 1555–1560.
- [16] L.X. Zhang, J.M. Shi, H.W. Li, X.Y. Tian, J.C. Feng, Interfacial microstructure and mechanical properties of ZrB₂-SiC-C ceramic and GH99 superalloy joints brazed with a Ti-modified FeCoNiCrCu high-entropy alloy. *Mater. Des.* 97 (2016) 230–238.
- [17] G. Wang, P. Xiao, Z.J. Huang, R.J. He. Brazing of ZrB₂-SiC ceramic with amorphous CuTiNiZr filler. *Ceram. Int.* 42(2016) 5130–5135.
- [18] Y.P. Liu, G. Wang, W. Cao, H.T. Xu, Z.J. Huang, D.D. Zhu, C.W. Tan. Brazing ZrB₂-SiC ceramics to Ti6Al4V alloy with TiCu-based amorphous filler. *J. Manuf. Processes.* 30 (2017) 516–522.
- [19] B. Cui, J.H. Huang, J.H. Xiong, H. Zhang, Reaction-composite brazing of carbon fiber reinforced SiC composite and TC4 alloy using Ag-Cu-Ti-(Ti + C) mixed powder, *Mater. Sci. Eng. A* 562(2013)203–210.
- [20] H. Chen, J. Peng, L. Fu, Effects of interfacial reaction and atomic diffusion on the mechanical property of Ti₃SiC₂ ceramic to Cu brazing joints, *Vacuum.* 130 (2016)56–62.
- [21] J.L. Qi, J.H. Lin, Y.H. Wan, L.X. Zhang, J. Cao, J.C. Feng, Joining of SiO₂-BN ceramic to Nb using a CNT-reinforced brazing alloy, *RSC. Adv.* 4 (2014) 64238–64243.
- [22] J.C. Feng, D. Liu, L.X. Zhang, X.C. Lin, P. He, Effects of processing parameters on microstructure and mechanical behavior of SiO₂/Ti-6Al-4V joint brazed with AgCu/Ni interlayer, *Mater. Sci. Eng. A* 527(2010)1522–1528.
- [23] Z.W. Yang, L.X. Zhang, Y.C. Chen, J.L. Qi, P. He, J.C. Feng, Interlayer design to control interfacial microstructure and improve mechanical properties of active brazed Invar/SiO₂-BN

- joint, *Mater. Sci. Eng. A* 575 (2013)199–205.
- [24] Q. Qiu, Y. Wang, Z. Yang, X. Hu, D. Wang, Microstructure and mechanical properties of TiAl alloy joint vacuum brazed with Ti-Zr-Ni-Cu brazing powder without and with Mo additive, *Mater. Des.* 90 (2016) 650–659.
- [25] X. Wang, L.F. Cheng, S.W. Fan, L.T. Zhang, Microstructure and mechanical properties of the GH783/2.5DC/SiC joints brazed with Cu-Ti+Mo composite filler, *Mater. Des.* 36 (2012) 499-504.
- [26] Y.X. Zhao, M.R. Wang, J. Cao, X.G. Song, D.Y. Tang, J.C. Feng, Brazing TC4 alloy to Si₃N₄ ceramic using nano-Si₃N₄ reinforced AgCu composite filler, *Mater. Des.* 76 (2015) 40-46.
- [27] A. A. Shirzadi, Y. Zhu, H. K. D. H. Bhadeshia, Joining ceramics to metals using metallic foam, *Mater. Sci. Eng. A* 496 (1-2) (2008) 501-506.
- [28] A. Junga, J. Luksch, S. Diebels, F. Schäfer, C. Motz. In-situ and ex-situ microtensile testing of individual struts of Al foams and Ni/Al hybrid foams, *Mater. Des.* 153 (2018) 104–119.
- [29] M.N. Feng, Y. Xie, C.F. Zhao, Z. Luo, Microstructure and mechanical performance of ultrasonic spot welded open cell Cu foam/Al joint, *J. Manuf. Processes.* 33 (2018) 86–95.
- [30] Z.Y. Wang, G. Wang, M.N. Li, J.H. Lin, Q. Ma, A.T. Zhang, Z.X. Zhong, J.L. Qi, J.C. Feng, Three-dimensional graphene-reinforced Cu foam interlayer for brazing C/C composites and Nb. *Carbon* 118 (2017) 723-730.
- [31] J. Ba, J.H. Lin, H.H. Wang, B.X. Qi, Z.X. Zhong, Z.Y. Wang, Q. Ma, J.L. Qi, J. Cao, J.C. Feng, Carbon nanotubes-reinforced Ni foam interlayer for brazing SiO₂-BN with Ti6Al4V alloy using TiZrNiCu brazing alloy, *Ceram. Int.* 44 (2018) 3684-3691.
- [32] L.X. Zhang, J.H. Yang, Z. Sun, X.P. Liu, J.C. Feng. Vacuum brazing Nb and BN-SiO₂ ceramic using a composite interlayer with network reinforcement architecture, *Ceram Int* 43 (2017) 8126-8132.
- [33] R.J. Sun, Y. Zhu, W. Guo, P. Peng, L.H. Li, Y. Zhang, J. Fu, F. Li, L.X. Zhang. Microstructural evolution and thermal stress relaxation of Al₂O₃/1Cr18Ni9Ti brazed joints with nickel foam. *Vacuum* 148 (2018) 18-26.
- [34] J.H. Lin, D.L. Luo, S.L. Chen, D.S. Mao, Z.Y. Wang, Q. Ma, J.L. Qi, J.C. Feng. Control interfacial microstructure and improve mechanical properties of TC4-SiO₂/SiO₂ joint by AgCuTi with Cu foam as interlayer. *Ceram. Int.* 42(2016) 16619-16625.
- [35] Y.T. Zhao, Y. Wang, Z.W. Yang, D.P. Wang. Relief of residual stress in Al₂O₃/Nb joints brazed with Ag-Cu-Ti/Cu/Ag-Cu-Ti composite interlayer. *Arch. Civ. Mech. Eng.* 19 (2019) 1-10.
- [36] W.Q. Yang, P. He, T.S. Lin, C.B. Song, R.S. Li, D.C. Jia, Diffusion bonding of ZrB₂-SiC and Nb using dynamic compressed Ni foam interlayer. *Mater. Sci. Eng. A* 573 (2013) 1–6.
- [37] T. Zaharinie, R. Moshwan, F. Yusof, M. Hamdi, T. Ariga. Vacuum brazing of sapphire with Inconel 600 using Cu/Ni porous composite interlayer for gas pressure sensor application, *Mater. Des.* 54 (2014) 375-381.
- [38] X.Y. Wang, C.L. Li, X.Q. Si, J.L. Qi, J.C. Feng, J. Cao. Brazing ZTA ceramic to TC4 alloy using the Cu foam as interlayer, *Vacuum* 155 (2018) 7-15.
- [39] Z.Y. Wang, M. N. Li, J. Ba, Q. Ma, Z.Q. Fan, J.H. Lin, Z.X. Zhong, J.L. Qi, J. Cao, J.C. Feng. In-Situ synthesized TiC nano-flakes reinforced C/C composite-Nb brazed joint. *J. Eur. Ceram. Soc.* 38 (2018) 1059-1068.

- [40] A.D. Cremasco, A.R. Messias, E.A.R. Esposito, R. Duek, Effects of alloying elements on the cytotoxic response of titanium alloys, *Mater. Sci. Eng. C* 31(2011) 833–839.
- [41] X. Dai, J. Cao, J. Liu, D. Wang, J. Feng, Interfacial reaction behavior and mechanical characterization of ZrO₂/TC4 joint brazed by Ag-Cu filler metal, *Mater. Sci. Eng. A* 646 (2015)182-189.
- [42] Z.R. Li, X.L. Xu, Z.Z. Wang, Interfacial product of ZrB₂-SiC brazing joint and growth kinetics of reaction layer. *J. Mater. Eng.* 12(2013) 44-48.
- [43] J. Lee, Y. Choi, J. Lee, G. Lee, M. Lee, C. Rhee, Low temperature brazing of titanium by the application of a Zr-Ti-Ni-Cu-Be bulk metallic glass alloy as a filler. *Intermetallics*. 18 (2010) 70-73.
- [44] M.F. Wu, M. Yang, C. Zhang, P. Yang, Research on the liquid phase spread-ing and microstructure of Ti/Cu eutectic reaction, *Trans. China. Weld. Inst.* 26 (2005) 68–71.
- [45] Y.X. Shen, Z.L. Li, C.Y. Hao, J.S. Zhang, A novel approach to brazing C/C composite to Ni-based superalloy using alumina interlayer, *J. Eur. Ceram. Soc.* 32 (2012) 1769-1774.
- [46] A. A. Shirzadi, Y. Zhu, H. K. D. H. Bhadeshi, Joining ceramics to metals using metallic foam, *Mater. Sci. Eng. A* 496 (2008) 501-506.
- [47] O.M. Akselsen, Advances in brazing of Ceramics, *J. Mater. Sci.* 27 (1992)1989-2000.
- [48] G. Wang, Y.J. Huang, M. Shagiev, J. Shen, Laser welding of Ti₄₀Zr₂₅Ni₃Cu₁₂Be₂₀ bulk metallic glass. *Mater. Sci. Eng. A*, 541 (2012) 33-37.
- [49] S.Y. Fu, B. Lauke, An analytical characterization of the anisotropy of the elastic modulus of misaligned short-fiber-reinforced polymers, *J. Compos. Sci. Technol.* 58 (1998) 389–400.
- [50] P.S. Turner, Thermal-Expansion Stresses in Reinforced Plastics. *J. Res. Natl. Bur. Stand* 37 (1946) 239-250.

Figure Captions

Fig.1 a) Microstructure of Cu foam, and b) schematic diagram of brazing assembly.

Fig. 2 a) Typical microstructure of ZS materials b) interfacial microstructure, and elemental distribution of c)Ti, d)Cu, e) Zr, f)Ni, g)Al, h)V, i)B, j)Si, k)C elements in the brazed joint.

Fig.3 SEM images of the brazed joint a) without Cu foam, b) with Cu foam, c) enlarged image of I zone, d) magnification images of II zone, and e) enlarged image of III zone.

Fig.4 Microstructural evolution of the ZS/TC4 brazed joints with Cu foam as interlayer: a) and b) the interaction between brazing filler and base materials; c) and d) the phase formation in the joint; e) the solidification stage of joint.

Fig.5 The shear strengths of the brazed joint as a function of brazing time.

Fig. 6 Interfacial microstructure of the ZS/TC4 brazed joints with Cu foam at 910°C for different holding times: a) 10 min; b) 20min, and c) 50 min.

Fig. 7 Fracture morphology of the brazed joints: a) without and b) with Cu foam.

Table Captions

Table 1 CTE of the ZrB₂-SiC ceramic at different temperatures.

Table 2 EDS of each point marked in Fig. 3.

Table 3 EDS of the blocky structure with different brazing parameters.